

Efimov Physics in Atom-Dimer Scattering of ${}^6\text{Li}$ Atoms

H.-W. Hammer,^{1,2} Daekyoung Kang,^{3,2} and Lucas Platter²

¹*Helmholtz-Institut für Strahlen- und Kernphysik
(Theorie) and Bethe Center for Theoretical Physics,
Universität Bonn, 53115 Bonn, Germany*

²*Institute for Nuclear Theory, University of Washington, Seattle WA 98195 USA*

³*Department of Physics, The Ohio State University, Columbus, OH 43210, USA*

(Dated: July 19, 2022)

Abstract

${}^6\text{Li}$ atoms in the three lowest hyperfine states display universal properties when the S-wave scattering length between each pair of states is large. Recent experiments reported four pronounced features arising from Efimov physics in the atom-dimer relaxation rate, namely two resonances and two local minima. We use the universal effective field theory to calculate the atom-dimer relaxation rate at zero temperature. Our results describe the four features qualitatively and imply there is a hidden local minimum. In the vicinity of the resonance at 685 G, we perform a finite temperature calculation which improves the agreement of theory and experiment. We conclude that finite temperature effects cannot be neglected in the analysis of the experimental data.

PACS numbers: 31.15.-p, 34.50.-s, 67.85.Lm, 03.75.Ss

Keywords: Degenerate Fermi gases, three-body recombination, scattering of atoms and molecules.

I. INTRODUCTION

Few-body systems with large two-body scattering length a are of great interest because they have universal properties insensitive to the details of the interaction at short distances. The simplest example is a universal two-body bound state with binding energy $\hbar^2/(ma^2)$ when $a > 0$. The corrections to this formula are suppressed by ℓ/a where ℓ is the natural low-energy length scale. For alkali atoms, ℓ is given by the van der Waals length ℓ_{vdW} which quantifies the range of the interaction. Examples of universal two-body states can be found in different branches of physics such as atomic physics, nuclear physics, and high-energy physics [1, 2]. Universal properties also exist for more than two particles. Systems of three identical bosons have an infinite number of geometrically spaced low-energy bound states (*Efimov trimers*) with an accumulation point at zero energy when the scattering length is taken to infinity and the range of the interaction is taken to zero [3]. In this so-called *unitary limit*, the binding energies of two successive trimers are related by a multiplicative factor of approximately $22.7^2 \approx 515$. This remarkable feature is the consequence of a discrete scaling symmetry with a scaling factor $e^{\pi/s_0} \approx 22.7$ where $s_0 \approx 1.00624$ for identical bosons. For more complicated systems, the scaling factor depends on the mass ratios and the spin of the components. We will refer to phenomena that result from the discrete scale invariance in the three-body sector as *Efimov physics* [4]. Corrections to Efimov physics in a process with typical wave number k are suppressed by ℓ/a and by ka .

Efimov trimers in ultracold atomic gases can be observed through enhanced loss rates in three-body recombination and atom-dimer relaxation processes [5–7]. The first evidence for an Efimov trimer in a system of bosonic ^{133}Cs atoms was presented by Kraemer *et al.* [8]. In a subsequent experiment with a mixture of ^{133}Cs atoms and dimers, Knoop *et al.* observed a resonance in the loss of atoms and dimers [9] which can be explained by an Efimov trimer crossing the atom-dimer threshold [10]. Efimov trimers have also been observed using other types of bosonic atoms. Zaccanti *et al.* [11] found evidence for two adjacent Efimov trimers in a gas of ultracold ^{39}K atoms and Gross *et al.* [12] measured two Efimov features across a Feshbach resonance and confirmed the universal relation between the features with ^7Li atoms. Attached to each Efimov trimer are two universal tetramers which can be observed in four-body loss processes [13–15]. Ferlaino *et al.* [16] observed signatures of two such tetramers close to an Efimov trimer with ^{133}Cs atoms. In ^7Li atoms, Pollack *et al.* [17] have seen two sets of two tetramers that are close to the corresponding Efimov trimers.

Efimov physics can also occur in fermionic systems with three or more spin states [3]. Several features associated with Efimov trimers in ^6Li atoms have been reported recently. Two three-body recombination features were observed by Ottenstein *et al.* [18] and Huckans *et al.* [19]. These features were analyzed theoretically in Refs. [20–22] and traced back to an Efimov trimer close to the three-atom threshold [21–23]. Another recombination feature was discovered by Williams *et al.* [24] and identified as a second trimer close to the threshold. Braaten *et al.* [23] analyzed the energy spectrum of Efimov trimers and predicted the crossings of the trimers with the atom-dimer threshold. These crossings imply two resonances in atom-dimer scattering. The resonances were identified in recent experiments by Lompe *et al.* [25] and Nakajima *et al.* [26]. Furthermore, two local minima in the atom-dimer relaxation rate were reported in Ref. [25].

In this paper, we study Efimov physics in atom-dimer scattering of ^6Li atoms and perform a complete zero-range calculation at zero temperature. The size of finite range corrections to our results is estimated. We identify the two resonances and the two minima in the

atom-dimer relaxation rate. Quantitatively, our zero temperature results show deviations from the data. An approximate finite temperature calculation near one of the resonances improves the description of the data considerably and shows that the discrepancy is largely due to finite temperature effects. The paper is organized as follows: In Sec. II and Sec. III we explain our theoretical framework. The numerical results at zero temperature are displayed and compared with the experimental data in Sec. IV. In Sec. V, we carry out an approximate finite temperature calculation near the resonance at $B = 685$ G. We summarize our results and conclude in Sec. VI.

II. DIMER RELAXATION

In this section we discuss the losses of atoms and dimers through inelastic scattering processes and present expressions for the relaxation rate constants.

Before proceeding with our discussion of atom-dimer scattering, we explain our notation and terminology. We label an atom in one of the three hyperfine states of the ${}^6\text{Li}$ atoms with an index i where $i = 1, 2$ or 3 . The S-wave scattering length between atoms in states i and j is denoted either as a_{ij} or as a_k where $k \neq i \neq j$. Two atoms in the same state can not scatter in an S-wave because of the Pauli principle. If the scattering length a_{ij} is positive and much larger than the van der Waals length $\ell_{\text{vdW}} \approx 65a_0$, the atoms i and j can form a dimer with binding energy $\hbar^2/(ma_{ij}^2)$. We call this dimer the (*shallow*) ij -dimer or simply a shallow dimer. Shallow dimers have to be distinguished from deep dimers with binding energy of order $\hbar^2/(m\ell_{\text{vdW}}^2)$ or larger.

In a gas of atoms i and jk -dimers, the atoms and dimers can undergo inelastic collisions into atoms and deeply bound dimers with a binding energy larger than that of the jk -dimer. This inelastic process is called *dimer relaxation*. The difference in the binding energies of the initial and final state dimers is released as kinetic energy and the atom and dimer in the final state recoil from each other. If their kinetic energies are larger than the trapping potential, they escape the trap. The loss rate for the number density n_i of atoms i and number density n_{jk} of jk -dimers is

$$\frac{d}{dt}n_i = \frac{d}{dt}n_{jk} = -\beta_i n_i n_{jk}, \quad (1)$$

where the coefficient β_i is the *relaxation rate constant* for the jk -dimer and atom i .

In the case of identical bosons, dimer relaxation is possible only if the final state consists of an atom and a deep dimer. However, in the three-fermion system relaxation can also occur into shallow dimers. For example, in a scattering process of an atom i and a jk -dimer, relaxation can proceed into the ij -dimer provided the binding energy of the ij -dimer is larger than that of the jk -dimer. Therefore, the total rate β_i is the sum of all relaxation rates into atoms plus shallow dimers and atoms plus deep dimers

$$\beta_i = \sum_{j \neq i} \beta_{i \rightarrow j}^{\text{sh}} + \beta_i^{\text{deep}}, \quad (2)$$

where the index i implies atom i plus jk -dimer in the initial state and the j implies atom j plus ik -dimer in the final state. For brevity, we refer to $\beta_{i \rightarrow j}^{\text{sh}}$ as the rate into the shallow dimer or the rate into the (final) ik -dimer and to β_i^{deep} as the rate into the deep dimers.

The relaxation rate can be calculated from the T-matrix element for atom-dimer scattering $\mathcal{T}_{ij}^{\text{AD}}(k, p; E)$ where k and p are the relative wave numbers of the atom and dimer in initial and final state, respectively, and E is the total energy. By using the *optical theorem*, we can calculate the total rate for atom-dimer scattering which is the sum of elastic and inelastic rates. However, in the low energy limit $k \rightarrow 0$, the elastic rate scales as k because $\mathcal{T}_{ii}^{\text{AD}}(k, k; E)$ is constant and the two-body phase space gives one power of k [4]. The elastic rate therefore vanishes at zero energy and the optical theorem gives the total relaxation rate β_i

$$\beta_i = \frac{2\hbar}{m} \text{Im} \mathcal{T}_{ii}^{\text{AD}}(0, 0, -1/(ma_i^2)). \quad (3)$$

The rate into the shallow dimer $\beta_{i \rightarrow j}^{\text{sh}}$ is determined by the square of the T-matrix element multiplied by the two-body phase space:

$$\beta_{i \rightarrow j}^{\text{sh}} = \frac{2p\hbar}{3\pi m} |\mathcal{T}_{ij}^{\text{AD}}(0, p, -1/(ma_i^2))|^2 \theta(a_i - a_j), \quad (4)$$

where the wave number $p = (2/\sqrt{3})\sqrt{a_j^{-2} - a_i^{-2}}$ and the θ -function is inserted because the relaxation is allowed only when the initial dimer binding energy is smaller than the final one. The prefactor $2p/(3\pi)$ comes from the two-body phase space integral.

The relaxation rate into deep dimers β_i^{deep} could also be calculated by using the T-matrix in a similar way to Eq. (4) if the theory described deep dimers explicitly. Alternatively, the effects of deep dimers can be taken into account indirectly by using an analytic continuation of the three-body parameter into the complex plane as introduced in Ref. [27]. Then, the partial rate β_i^{deep} can be obtained by using the relation in Eq. (2).

III. STM EQUATION

The Skorniakov–Ter-Martirosian (STM) equation [28] is an integral equation that describes three-atom scattering interacting through zero-range interactions. In this section, we discuss the STM equation and relate the T-matrix element $\mathcal{T}_{ij}^{\text{AD}}$ to the amplitude \mathcal{A}_{ij} that is the solution to the STM equation.

We consider only the S-wave contribution and assume that higher partial wave contributions are suppressed at low temperature. For the three-fermion system, the STM equation forms 9 coupled equations for the amplitudes $\mathcal{A}_{ij}(k, p; E)$ [20, 23]. For non-zero energy, the equation is given by

$$\begin{aligned} \mathcal{A}_{ij}(k, p; E) &= (1 - \delta_{ij}) Q(k, p; E) \\ &+ \frac{2}{\pi} \sum_k (1 - \delta_{kj}) \int_0^\Lambda dq q^2 Q(q, p; E) D_k(q; E) \mathcal{A}_{ik}(k, q; E), \end{aligned} \quad (5)$$

where $\mathcal{A}_{ij}(k, p; E)$ is the amplitude for an atom i and a complementary pair of atoms to scatter into an atom j and a complementary pair and Λ is an ultraviolet cutoff. The function $Q(k, p; E)$ and the 2-atom propagator $D_k(q; E)$ are given by

$$Q(k, p; E) = \frac{1}{2kp} \log \left[\frac{k^2 + kp + p^2 - mE - i\epsilon}{k^2 - kp + p^2 - mE - i\epsilon} \right], \quad (6)$$

$$D_k(q; E) = \frac{1}{-1/a_k + \sqrt{\frac{3}{4}q^2 - mE - i\epsilon}}. \quad (7)$$

The solutions of the STM equation (6) depend log-periodically on Λ with a discrete scaling factor $e^{\pi/s_0} \approx 22.7$, where $s_0 \approx 1.00624$. The dependence on the arbitrary cutoff Λ can be eliminated in favor of a physical 3-body parameter such as the binding wave number of an Efimov trimer in the unitary limit. For convenience, we choose to work directly with the wave number cutoff Λ in our calculations. If deep dimers are present, the trimer has a finite width that allows it to decay into an atom and a deep dimer. The effects of deep dimers can be taken into account by analytically continuing the cutoff Λ into the complex plane [27]

$$\Lambda \rightarrow \Lambda e^{i\eta_*/s_0}, \quad (8)$$

where η_* is a width parameter associated with the effects of the deep dimers. Λ and η_* are determined from experimental measurements of three-body recombination in the ${}^6\text{Li}$ system [24] and their numerical values are $\Lambda = 456 a_0^{-1}$ and $\eta_* = 0.016$ [23] where a_0 is the Bohr radius.

In order to obtain the T-matrix element, the amplitude \mathcal{A}_{ij} must be multiplied with the dimer-wavefunction renormalization factors $\sqrt{Z_i Z_j}$, where $Z_i = 8\pi/a_i$,

$$\mathcal{T}_{ij}^{\text{AD}}(k, p; E) = \frac{8\pi}{\sqrt{a_i a_j}} \mathcal{A}_{ij}(k, p; E). \quad (9)$$

By solving the STM equation (6) and using the relation in Eq. (9), we can calculate the relaxation rates in Eqs. (3) and (4).

IV. ZERO TEMPERATURE RESULTS

In this section we present our numerical results for the dimer relaxation rate constants β_i at zero temperature and compare them with recent measurements in Refs. [25, 26]. We solve the STM equation in Eq. (6) numerically with 5 input parameters: the three pair scattering lengths a_i , $i = 1, 2, 3$, the cutoff Λ and the width parameter η_* . We use the values $\Lambda = 456 a_0^{-1}$ and $\eta_* = 0.016$ that have been determined from measurements of the three-body recombination rate in Ref. [24] and have been used in Ref. [23] to predict the atom-dimer relaxation rate.

Fig. 1 shows the scattering lengths for the 3 lowest hyperfine state of ${}^6\text{Li}$ as a function of the magnetic field. The atom-dimer relaxation rate β_i is non-zero in the region of positive scattering length a_i . The upper limit of the region is set by the Feshbach resonances at 811 G, 690 G, and 834 G for a_1 , a_2 , and a_3 , respectively. If the scattering length is much larger than the van der Waals length $\ell_{\text{vdW}} \approx 65a_0$, the universal theory is valid. We denote this region as the *universal region*. Corrections due to the finite range of the interaction should be small in the universal region. In practice, we apply the universal zero-range theory when all scattering lengths are at least two times larger than ℓ_{vdW} corresponding to magnetic fields $B > 608$ G. The expected error due to finite range corrections is ℓ_{vdW}/a and therefore smaller than 50% in this region.

In Ref. [23], two crossings of Efimov trimers with the atom-dimer threshold have been predicted. Both are located at the 1(23)-threshold: at $B_* = 672$ G and at $B'_* \approx 597$ G. Here the index 1 denotes the atom and the index (23) the dimer. Since the atom-dimer relaxation is resonant when the trimer appears near the threshold, two resonances are expected in the rate β_1 near B_* and B'_* . The resonance at B_* is well in the universal region where all scattering lengths are much larger than ℓ_{vdW} while B'_* is slightly outside. Therefore, the

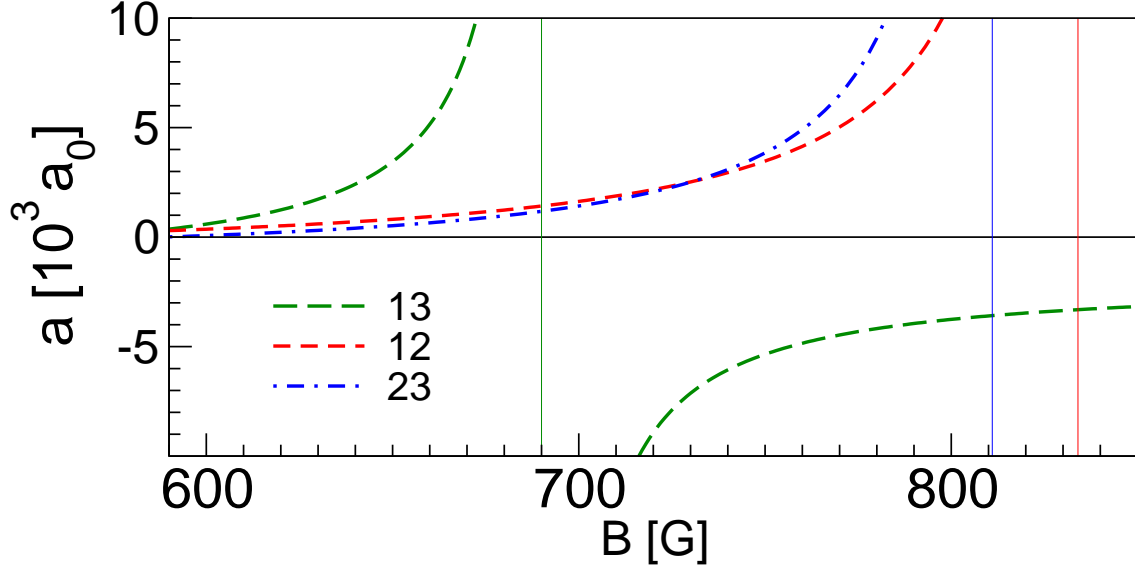


FIG. 1: (Color online) The scattering lengths for the three lowest hyperfine states of ${}^6\text{Li}$ in units of $10^3 a_0$ as a function of the magnetic field B from [29]: $a_{13} \equiv a_2$ (long-dashed), $a_{12} \equiv a_3$ (short-dashed), and $a_{23} \equiv a_1$ (dashed-dotted). The vertical lines at 690 G, 811 G, and 834 G indicate the Feshbach resonances for a_{13} , a_{23} , and a_{12} , respectively.

resonance position B_* should be accurately determined with corrections of order $\ell_{\text{vdW}}/a_{23} \approx 10\%$ where the value of a_{23} at the resonance was used. The position B'_* is outside the universal region and can receive large non-universal corrections of order 100%. These error estimates are accurate up to a prefactor of order one. The exact value of this prefactor can only be obtained from an explicit calculation of the range corrections. Note also that these percentage errors apply to the positions in terms of the scattering length. To obtain the errors for the corresponding magnetic field they have to be converted using Fig. 1.

In Fig. 2, we show our numerical results for β_1 and compare them with the recent measurements of Refs. [25, 26]. We give the full relaxation rate as well the individual contributions from shallow and deep dimers. In the magnetic field region from 590 G to 730 G, only the relaxation into deep dimers contributes to β_1 since the energy of the 23-dimer is larger than the energy of the other shallow dimers. At a magnetic field of 730 G, the 23-dimer crosses the 12-dimer and the relaxation channel into 12-dimers opens up. At 811 G, the 23-dimer disappears through the three-atom threshold and the relaxation rate vanishes.

Our results show two resonances at $B_* = 672$ G and $B'_* \approx 597$ G. There is also a dramatic change in the relaxation rate at 730 G because the relaxation channel into 12-dimers opens and the corresponding rate into the 12-dimer increases rapidly. Our results describe the resonances in the experimental data qualitatively. The second resonance has been measured at $B_*^{\text{exp}} = 685$ G in Ref. [25, 26]. This value is 13 G away from the theoretical prediction $B_* = 672$ G. In terms of the scattering length, this corresponds to $a_{23}(B_*^{\text{exp}})/a_{23}(B_*) = 1076/835 \approx 1.3$, leading to a 30% shift in the resonance position. This shift is a factor three larger than the naive error estimate of 10%. Taking into account the unknown prefactor of order one in the estimate, however, the two values are consistent. Except near the resonance, the experimental data are generally above our results.

Lompe *et al.* [25] analyzed their data near the resonance at B_* using an approximate

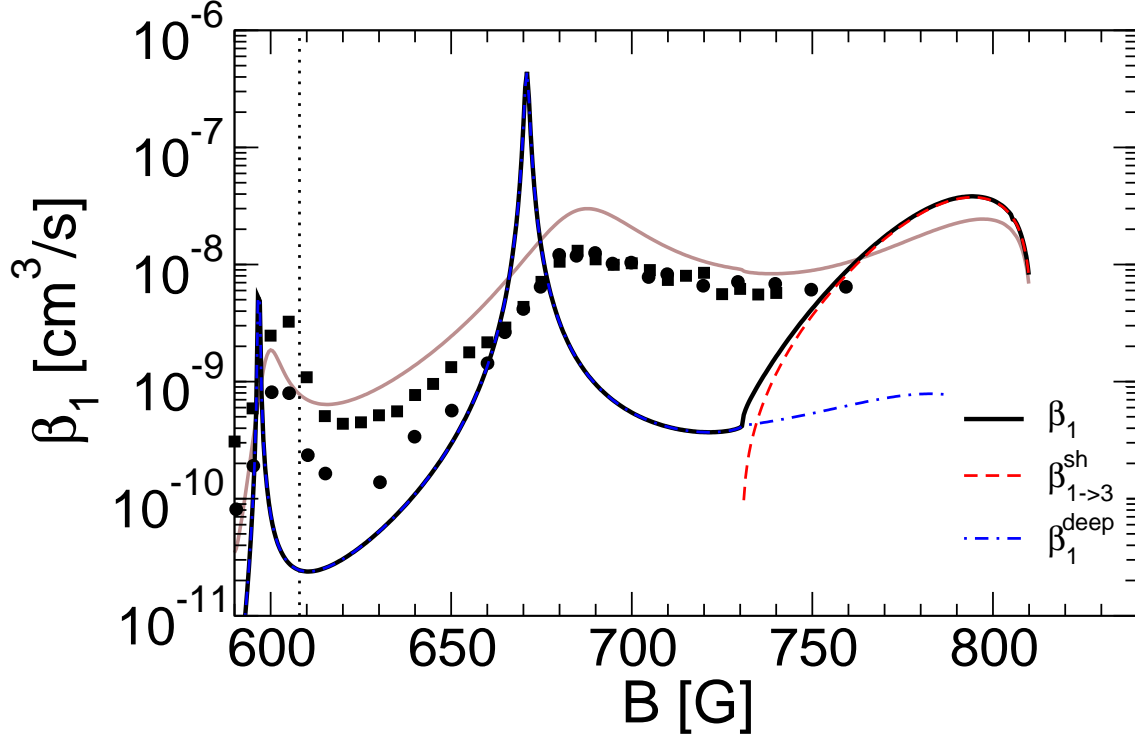


FIG. 2: (Color online) The relaxation rate constant for the 23-dimer and atom 1 as a function of the magnetic field B . The squares and circles are data points from Ref. [25] and Ref. [26], respectively. The curves are our results for the total rate β_1 (solid line), the partial rate into atom 3 and the 12-dimer $\beta_{1 \rightarrow 3}^{\text{sh}}$ (dashed line), and the rate into an atom and a deep dimer β_1^{deep} (dashed-dotted line). The light solid line gives the total rate β_1 for the parameters obtained in Ref. [25] while the vertical line marks the boundary of the universal region.

analytic expression from [23] and extracted the resonance position and the width parameter η_* . They found the value $\eta_* = 0.34$ which is more than an order of magnitude larger than the value 0.016 extracted from three-body recombination. Moreover, the normalization of the relaxation rate was adjusted to describe the data. The light solid curve in Fig. 2 gives our universal result for the parameters $\Lambda = 329 a_0^{-1}$ (which reproduces the resonance position $B_*^{\text{exp}} = 685$ G) and $\eta_* = 0.34$. These parameters give a much better description of the data in Refs. [25, 26] but are generally a factor 2-3 above the experimental data. However, one should keep in mind that the experimental data are only a factor three lower than the unitarity bound and finite temperature effects are likely important. We will come back to this issue in the next section.

The reason for the considerably larger value of η_* extracted in [25] compared to the value from recombination data is not understood. However, we note that a similar discrepancy between the values of η_* from atom-dimer relaxation and three-body recombination occurs in the bosonic system of ^{133}Cs atoms [9, 10].

Nakajima *et al.* [26] performed a numerical analysis for β_1 based on the universal theory and on a two-channel model. Their results obtained with the universal theory agree with our calculation. Within the two-channel model they derived energy-dependent scattering lengths which introduce non-universal effects in the two-body amplitudes. Because this model cannot resolve the discrepancy between the universal results and the measurements

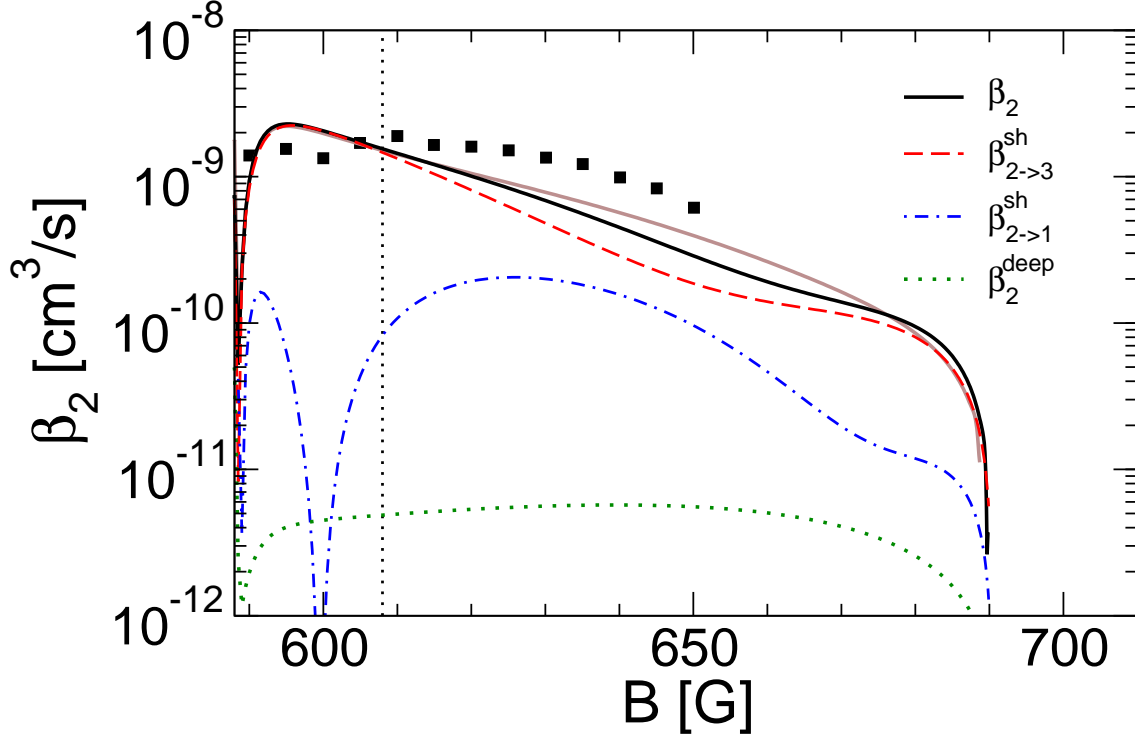


FIG. 3: (Color online) The relaxation rate constant for the 13-dimer and atom 2 as a function of the magnetic field B . The squares are data points from Ref. [25]. The curves are our results for the total rate β_2 (solid line) and the partial rates into an atom 3 and a 12-dimer $\beta_{2 \rightarrow 3}^{\text{sh}}$ (dashed line), into an atom 1 and a 23-dimer $\beta_{2 \rightarrow 1}^{\text{sh}}$ (dashed-dotted line), and into an atom and a deep dimer β_2^{deep} (dotted line). The light solid line gives the total rate β_1 for the parameters obtained in Ref. [25] while the vertical line marks the boundary of the universal region.

they concluded that the three-body parameters Λ and η_* depend on the magnetic field.

In Fig. 3, we show the experimental data from Ref. [25] and our numerical results for β_2 . The total rates, both of the data and the numerical results, show no pronounced structure. However, there is a local minimum in the partial rate $\beta_{2 \rightarrow 1}^{\text{sh}}$ near 600 G that is outside the universal region. As discussed in Ref. [30], this minimum is the effect of destructive interference between different recombination channels. This interference pattern does not exist in systems with identical bosons where relaxation can occur only into deep dimers. In the total rate, the interference is hidden by the dominant process $\beta_{2 \rightarrow 3}^{\text{sh}}$. The light solid curve again gives our universal result for the parameters $\Lambda = 329 a_0^{-1}$ and $\eta_* = 0.34$ obtained in Ref. [25]. The difference between the two parameter sets is very small for β_2 , but the alternative set gives a slightly better description of the data.

Fig. 4 shows our results and the recent measurement [25] for β_3 . Between 590 G and 730 G, the energy of the 12-dimer is smaller than the energy of the 23-dimer and the relaxation channel into 23-dimers is open. After the 23-dimer crosses the 12-dimer at 730 G this relaxation channel is closed and only relaxation into deep dimers is possible. Two interference minima have been observed at 610 G and 695 G [25] while our results show two minima at 600 G and 715 G. Above 700 G, the data are larger than our results by more than a factor 10. Using the alternative parameters $\Lambda = 329 a_0^{-1}$ and $\eta_* = 0.34$ obtained in Ref. [25], we again find a better agreement with the data. [[With these parameters the

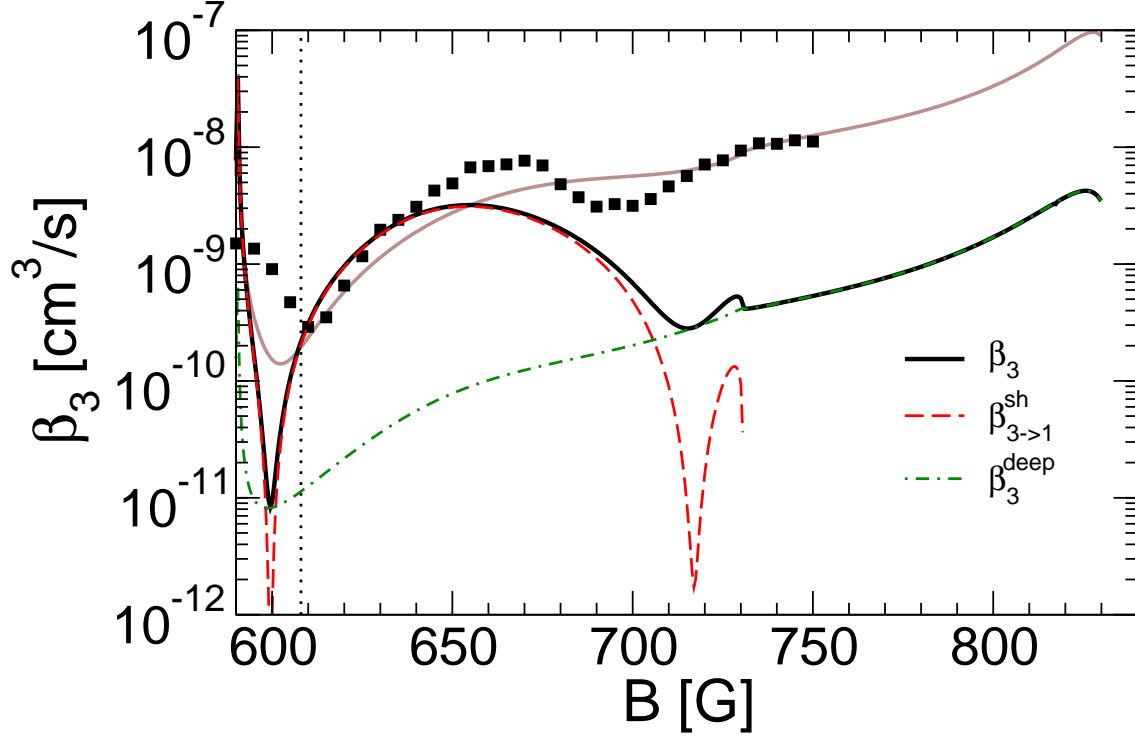


FIG. 4: (Color online) The relaxation rate constant for the 12-dimer and atom 3 as a function of the magnetic field B . The squares are data points from Ref. [25]. The curves are our results for the total rate β_3 (solid line), the partial rate into atom 1 and a 23-dimer $\beta_{3 \rightarrow 1}^{\text{sh}}$ (dashed line), and the rate into an atom and a deep dimer β_3^{deep} (dashed-dotted line). The light solid line gives the total rate β_1 for the parameters obtained in Ref. [25] while the vertical line marks the boundary of the universal region.

second minimum in the rate into the shallow dimer disappears beyond 730 G hence, the partial rate decreases monotonically and vanishes near 730 G. For smaller η_* the position of the minimum in the total rate is around 730 G. As η_* increases the position remains almost the same and the depth of the minimum becomes shallower. The minimum is not visible when $\eta_* = 0.34$ because the rate into deep dimers is much larger than the rate into the shallow dimer. Therefore, with these parameters that were fit to data for β_1 the position of the second minimum in the data for β_3 cannot be explained correctly.]

If the rate into 23-dimers could be separated experimentally from the total rate, it would clearly determine the positions of the local minima. This could be achieved by tuning the depth of trapping potential such that it is much larger than the kinetic energies of atoms and 23-dimers in the final state but much smaller than the energies of atoms and deep dimers in the final state. The kinetic energies of an atom and a deep dimer in the final state could be estimated from the binding energy of the deep dimers. Their energies would be of the order of the van der Waals energy or larger: $E_{\text{vdW}}/\hbar \approx 154$ MHz, where $E_{\text{vdW}} = \hbar^2/(m\ell_{\text{vdW}}^2)$.¹ The kinetic energies of an atom and a 23-dimer are given by the difference in binding energies between the 12-dimer and the 23-dimer: $\hbar/(2\pi m)(a_{23}^{-2} - a_{12}^{-2})$ is about 1 MHz at 650 G and

¹ A convenient conversion constant for ^6Li atoms is given by $\hbar^2/(ma_0^2) = 600h$ GHz = $28.8k_B$ K.

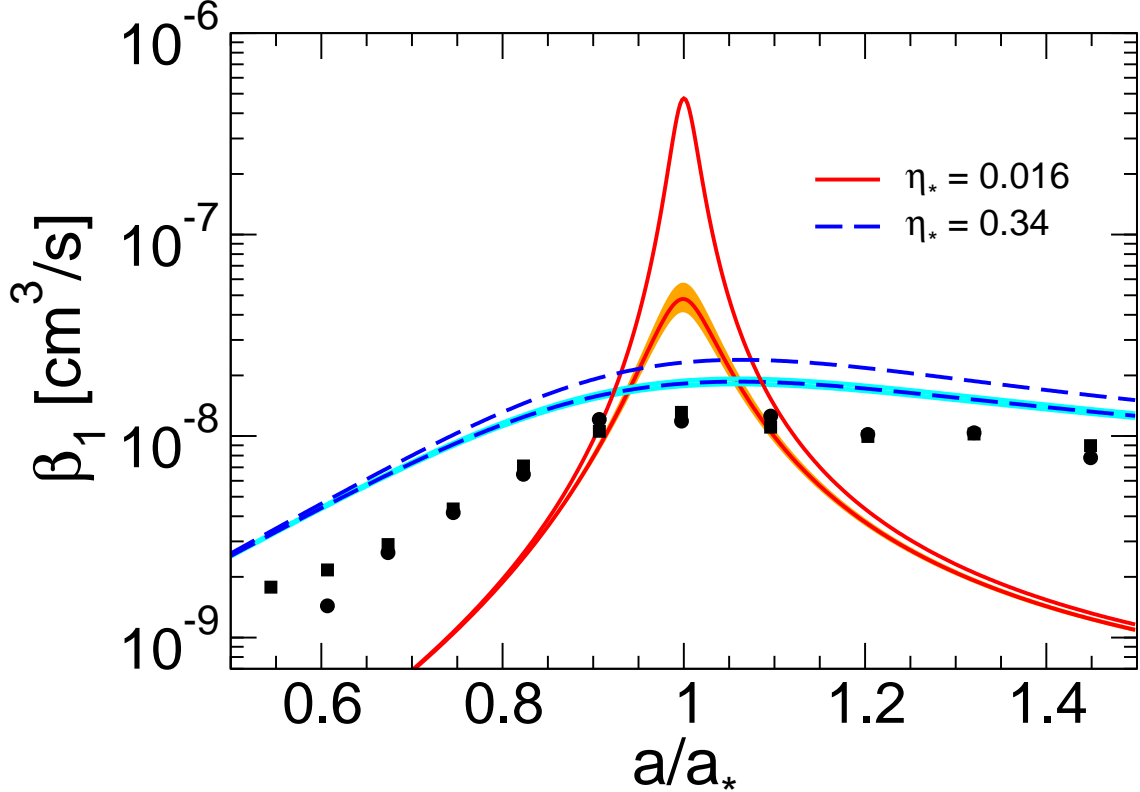


FIG. 5: (Color online) The relaxation rate constant β_1 for a 23-dimer and an atom 1 as a function of a/a_* near the resonance at $B_*^{\text{exp}} = 685$ G ($a_* = 1076 a_0$). Squares and circles are data points from Ref. [25] and Ref. [26], respectively. The solid (dashed) curves correspond to $\eta_* = 0.016$ ($\eta_* = 0.34$). The upper curves give the zero temperature result, while the lower curves give the finite temperature result for $T = 60 \pm 15$ nK with the shaded area indicating the temperature uncertainty.

vanishes at 730 G. This way one may be able to measure the rate into deep dimers separately and to extract the rate into the 23-dimer.

V. FINITE TEMPERATURE RESULTS

The results from the previous section suggest that finite temperature effects may play an important role in understanding the atom-dimer relaxation data from Refs. [25, 26]. A full finite temperature calculation of the ^6Li system is beyond the scope of this work. Therefore, we perform an approximate calculation of the relaxation rate β_1 near the resonance at $B_*^{\text{exp}} = 685$ G.

We start from the approximate expression for the scattering length between an atom 1 and a 23-dimer near the resonance at B_* that was extracted from a calculation of the trimer binding energy in [23]:

$$a_{1(23)} \approx (C_1 \cot[s_0 \ln(a_{23}/a_*) + i\eta_*] + C_2) a_{23}, \quad (10)$$

where $a_* = a_{23}(B_*)$ and the coefficients are $C_1 = 0.67$ and $C_2 = 0.65$. Using the scattering

length approximation for the S-wave atom-dimer scattering amplitude in the 1(23)-channel,

$$f_{1(23)}(k) = [-1/a_{1(23)} - ik]^{-1}, \quad (11)$$

we can calculate the inelastic scattering cross section. At low temperatures, the contributions from higher partial waves can be neglected. We subtract the elastic cross section from the total cross section obtained via the optical theorem as in [31] and find for the inelastic cross section:

$$\sigma_{1(23)}^{(inelastic)}(k) = \frac{4\pi}{k} \frac{-\text{Im } a_{1(23)}}{1 - 2k\text{Im } a_{1(23)} + k^2|a_{1(23)}|^2}. \quad (12)$$

The total dimer-relaxation rate β_1 can then be calculated by taking a Boltzmann thermal average of the inelastic reaction rate $v_{rel} \sigma_{1(23)}^{(inelastic)}(k)$ where $v_{rel} = 3\hbar k/(2m)$ is the relative velocity of the atom and dimer in the initial state. This leads to the expression

$$\beta_1(T) = \frac{3\hbar}{2m} \langle k \sigma_{1(23)}^{(inelastic)}(k) \rangle = \frac{3\hbar}{2m} \frac{3\lambda_T^3}{4\pi^2} \sqrt{\frac{3}{2}} \int_0^\infty k^2 dk k \sigma_{1(23)}^{(inelastic)}(k) e^{-\frac{3\hbar^2 k^2}{4mk_B T}}, \quad (13)$$

where $\lambda_T = \sqrt{2\pi\hbar^2/(mk_B T)}$ is the thermal de Broglie wavelength of the atoms.

Our results for the atom-dimer relaxation rate constant near the resonance at $B_*^{\text{exp}} = 685$ G are shown in Fig. 5. The results for the width parameters $\eta_* = 0.016$ and $\eta_* = 0.34$ are given by the solid and dashed curves, respectively. In each case the upper curves give the zero temperature result while the lower curves give the finite temperature result for $T = 60 \pm 15$ nK. Here, the shaded area indicates the uncertainty from the temperature. The value of $a_* = 1076 a_0$ has been fixed to reproduce the resonance position at $B_*^{\text{exp}} = 685$ G. For $\eta_* = 0.016$, the finite temperature effects decrease the height of the peak by an order of magnitude but the predicted resonance shape is still much narrower than the data. The finite temperature effects are much less severe for $\eta_* = 0.34$. They only lead to a reduction of β_1 by about a factor of two but clearly improve the description of the data. We conclude that finite temperature effects can not resolve the question of the different values for η_* in the three-body recombination and dimer-relaxation data. Moreover, while finite temperature effects are important, a qualitative description of the data at $T \approx 60$ nK can be already achieved with a zero temperature calculation.

VI. SUMMARY AND OUTLOOK

In this work, we have studied Efimov physics in atom-dimer relaxation of ^6Li atoms in the three lowest hyperfine states using the universal zero-range theory. Two resonances were observed at magnetic fields 603 G and 685 G in the relaxation rate β_1 in recent experiments [25, 26]. These resonances are consequences of two Efimov trimers close to the atom-dimer threshold. Their positions have been predicted by Braaten *et al.* [23]. The measured position of the resonance at 685 G [25, 26], which is well within the universal region, is larger than the prediction by about 30%. This is consistent with an error of order 10% error due to effective range corrections. However, the value $\eta_* = 0.016$ extracted from the three-body recombination data is not able to describe the atom-dimer relaxation data which require the larger value $\eta_* = 0.34$ [25]. The reason for the larger value of η_* in dimer relaxation compared to the value from recombination data is not understood. However, we note that

a similar discrepancy between the values of η_* from atom-dimer relaxation and three-body recombination occurs in the bosonic systems of ^{133}Cs atoms [9, 10].

Using the value $\eta_* = 0.34$, our zero temperature calculation is able to describe the data qualitatively. In the vicinity of this resonance, we have also performed an approximate finite temperature calculation and find sizable temperature effects that can suppress the relaxation rate by an order of magnitude if $\eta_* = 0.016$. For the larger value $\eta_* = 0.34$, however, these effects lead to a moderate suppression of about a factor of two, such zero temperature results are useful as a first approximation.

In Ref. [25], also two local minima at 610 G and 695 G are discovered in the rate β_3 . Those minima can be associated with destructive interference between different recombination channels [30]. Our numerical results show that the partial rate into 23-dimers is responsible for the minima but the positions of the minima are displaced by -10 G and +20 G from the measurements. These displacements correspond to a 30% shift in terms of the scattering length compared to our predictions. Since the scattering length, a_{23} , is about a factor two larger in this magnetic field region than around the resonance in β_1 , one would expect smaller corrections here. The observed shifts indicate that the destructive interference leading to the minima might be dominated by wave numbers k larger than $1/a_{23}$ such that corrections of order $k\ell_{v,dW}$ are important. Moreover, finite temperature effects could fill the minima in an asymmetric fashion. The total rate β_2 shows no structure. However, the partial rate into the 23-dimer shows a local minimum near 600 G. In the total rate this feature is hidden by the dominant rate into the 12-dimer.

In order to better understand the discrepancy between the values of η_* and the resonance positions extracted from three-body recombination and atom-dimer relaxation two important improvements are required in a future analysis. First, a full finite temperature calculation of atom-dimer relaxation should be carried out. This requires calculating atom-dimer scattering above the dimer breakup thresholds and in higher partial waves. Due to the different pair scattering lengths in the three channels, such a calculation is considerably more complex than in the case of identical bosons [32]. However, it will allow to better distinguish effects from the resonance width parameter η_* and from the finite temperature which can be partially traded for each other [10, 32]. Second, an analysis of the effective range corrections should be performed in order to describe the observed shifts in the resonance positions quantitatively. A similar analysis for systems of identical bosons was carried out in Refs. [33, 34].

Acknowledgments

We thank Eric Braaten, Selim Jochim, and Thomas Lompe for discussions and Selim Jochim for providing their experimental results. We acknowledge the INT program ‘‘Simulations and Symmetries: Cold Atoms, QCD, and Few-hadron Systems’’, during which this work was initiated. This work was supported in part by a joint grant from AFOSR and ARO, by the BMBF under contract 06BN9006 and by DOE grant DE-FG02-00ER41132.

-
- [1] H.-W. Hammer and L. Platter, arXiv:1001.1981 [nucl-th].
 - [2] L. Platter, *Few Body Syst.* **46**, 139 (2009).

- [3] V. Efimov, Phys. Lett. **33B**, 563 (1970); Nucl. Phys. A **210**, 157 (1973).
- [4] E. Braaten and H.-W. Hammer, Phys. Rept. **428**, 259 (2006).
- [5] E. Nielsen and J.H. Macek, Phys. Rev. Lett. **83**, 1566 (1999).
- [6] B.D. Esry, C.H. Greene, and J.P. Burke, Phys. Rev. Lett. **83**, 1751 (1999).
- [7] P.F. Bedaque, E. Braaten, and H.-W. Hammer, Phys. Rev. Lett. **85**, 908 (2000).
- [8] T. Kraemer, M. Mark, P. Waldburger, J.G. Danzl, C. Chin, B. Engeser, A.D. Lange, K. Pilch, A. Jaakkola, H.-C. Nägerl, and R. Grimm, Nature **440**, 315 (2006).
- [9] S. Knoop, F. Ferlaino, M. Mark, M. Berninger, H. Schoebel, H.-C. Naegerl, and R. Grimm, Nature Physics **5**, 227 (2009).
- [10] K. Helfrich and H.-W. Hammer, Europhys. Lett. **86**, 53003 (2009).
- [11] M. Zaccanti, B. Deissler, C. D’Errico, M. Fattori, M. Jona-Lasinio, S. Müller, G. Roati, M. Inguscio, and G. Modugno, Nature Physics **5**, 586 (2009).
- [12] N. Gross, Z. Shotan, S. Kokkelmans, L. Khaykovich, Phys. Rev. Lett. **103**, 163202 (2009).
- [13] L. Platter, H.-W. Hammer and U. G. Meißner, Phys. Rev. A **70**, 052101 (2004).
- [14] H.-W. Hammer and L. Platter, Eur. Phys. J. A **32**, 113 (2007).
- [15] J. von Stecher, J. P. D’Incao, and C. H. Greene, Nature Physics **5**, 417 (2009).
- [16] F. Ferlaino, S. Knoop, M. Berninger, W. Harm, J. P. D’Incao, H.-C. Nägerl, R. Grimm, Phys. Rev. Lett. **102**, 140401 (2009).
- [17] S. Pollack, D. Dries, and R. Hulet, Science **326**, 1683 (2009).
- [18] T.B. Ottenstein, T. Lompe, M. Kohnen, A.N. Wenz, and S. Jochim, Phys. Rev. Lett. **101**, 203202 (2008).
- [19] J.H. Huckans, J.R. Williams, E.L. Hazlett, R.W. Stites, and K.M. O’Hara, Phys. Rev. Lett. **102**, 165302 (2009).
- [20] E. Braaten, H.-W. Hammer, D. Kang and L. Platter, Phys. Rev. Lett. **103**, 073202 (2009).
- [21] R. Schmidt, S. Floerchinger and C. Wetterich, Phys. Rev. A **79**, 053633 (2009).
- [22] P. Naidon, M. Ueda, Phys. Rev. Lett. **102**, 073203 (2009)
- [23] E. Braaten, H.-W. Hammer, D. Kang and L. Platter, Phys. Rev. A **81**, 013605 (2010).
- [24] J. R. Williams, E. L. Hazlett, J. H. Huckans, R. W. Stites, Y. Zhang and K. M. O’Hara, Phys. Rev. Lett. **103**, 130404 (2009).
- [25] T. Lompe, T. B. Ottenstein, F. Serwane, K. Viering, A. N. Wenz, G. Zürn and S. Jochim, [arXiv:1003.0600v1 [cond-mat.quant-gas]].
- [26] S. Nakajima, M. Horikoshi, T. Mukaiyama, P. Naidon and M. Ueda, [arXiv:1003.1800v1 [cond-mat.quant-gas]].
- [27] E. Braaten, H.-W. Hammer and M. Kusunoki, Phys. Rev. A **67**, 022505 (2003).
- [28] G.V. Skorniakov and K.A. Ter-Martirosian, Sov. Phys. JETP **4**, 648 (1957).
- [29] P.S. Julienne, private communication.
- [30] J. P. D’Incao and B. D. Esry, Phys. Rev. Lett. **103**, 083202 (2009).
- [31] E. Braaten and H.-W. Hammer, Phys. Rev. A **75**, 052710 (2007); Erratum: Phys. Rev. A **79**, 039905(E) (2009).
- [32] E. Braaten, H.-W. Hammer, D. Kang and L. Platter, Phys. Rev. A **78**, 043605 (2008).
- [33] H.-W. Hammer, T. A. Lahde and L. Platter, Phys. Rev. A **75**, 032715 (2007).
- [34] C. Ji, L. Platter and D. R. Phillips, arXiv:1005.1990 [cond-mat.quant-gas].